ARCHIVIO ISTITUZIONALE
DELLA RICERCA

Alma Mater Studiorum Università di Bologna
Archivio istituzionale della ricerca

PWI and DWI Systems in Modern GDI Engines: Optimization and Comparison Part I: Non-Reacting Flow Analysis

This is the final peer-reviewed author's accepted manuscript (postprint) of the following publication:

Published Version:
Falfari S., Cazzoli G., Ricci M., Forte C. (2021). PWI and DWI Systems in Modern GDI Engines: Optimization and Comparison Part I: Non-Reacting Flow Analysis. SAE International [10.4271/2021-01-0461].

Availability:
This version is available at: https://hdl.handle.net/11585/862239 since: 2022-02-21

Published:
DOI: http://doi.org/10.4271/2021-01-0461

Terms of use:

Some rights reserved. The terms and conditions for the reuse of this version of the manuscript are specified in the publishing policy. For all terms of use and more information see the publisher's website.

This item was downloaded from IRIS Università di Bologna (https://cris.unibo.it/).
When citing, please refer to the published version.

(Article begins on next page)

06 May 2026

2021-01-0461

PWI and DWI Systems in Modern GDI Engines: Optimization and Comparison Part I: Non-Reacting Flow Analysis

S. Falfari, G. Cazzoli
University of Bologna
M. Ricci, C. Forte
NAIS s.r.l.

Copyright © 2019 SAE International

Abstract

Currently engine designers are focusing their attention on the improvement of the engine efficiency, led by the reduction of in-cylinder temperature and the adoption of stoichiometric combustion in the full range of the engine operation map. The most demanding points are those close to full power: water injection is thought to help in fulfilling this goal, thus contributing towards more efficient engines. To perform a rapid optimization of the main parameters involved by the water injection process, it is necessary to have reliable CFD methodologies capable of capturing the most important phenomena. In the present work, a methodological approach based on the CFD simulation of non-reacting flows of S.I. GDI turbocharged engines under water injection operation is pursued using AVL Fire code v. 2020. Port Water Injection (PWI) and Direct Water Injection (DWI) have been tested for the same baseline engine configuration and they have been run at full power condition, at the same rated power engine speed by varying: i) the injection pressure; ii) the injection timing (water injection phasing has significant effect on the water evaporation rate and on its impact on walls); iii) the normalized water injected mass on the stoichiometric fuel mass. The main results have been checked in terms of evaporation rate, cooling temperature, and efficiency, also considering the mixture quality and the fluid-dynamics aspects, in particular the possible degeneration of the turbulence level during the water injection process. The main aim of these simulations is to maximize water injection benefits and minimize possible disadvantage, such as primarily oil dilution and incomplete water evaporation to reduce water tank volume and refilling frequency. Water injection has demonstrated to allow to adopt higher compression ratio with limited penalties on performance. Therefore, for pursuing the target of improving the engine efficiency over the whole engine map and maintaining good performance level, the geometric compression ratio of the baseline engine has been increased. The adopted CFD methodology has shown to be able to capture the thermodynamic effects of water injection.

Introduction

CO_2 emissions reductions and development of technologies aimed to increase engine efficiency are the current guidelines for new engine concept design. During the transition from the current mobility to a new sustainable concept, future projections show that 80% of vehicles in the next decade still rely on internal combustion engines [1]. Thus, the new scenario for automotive application is affected mostly by two distinct aspects, which become synergic in their application in future engines:

I. The future limits to the global CO_2 emissions (car engines are responsible of around 12% of total EU emission of carbon dioxide) together with the necessity of a further reduction of the fossil non-renewable fuels have moved the automotive engine research towards new solutions. The designers are focusing their attention on both the drop of passive resistances and the improvement of the engine efficiency for reducing the fuel consumption. As far as the last issue is concerned, many gasoline engine technologies for fuel economy improvement have been identified: i) Gasoline Direct Injection; ii) Downsizing and Turbocharging; iii) Variable Valve Timing (VVT); iv) Variable Valve Actuation (VVA); v) Exhaust Gas Recirculation (EGR); vi) Variable Compression Ratio (VCR); vii) Water Injection. Downsizing and turbocharging are strictly related by the necessity of maintaining a proper torque output. Therefore, high boost level is necessary but involving the risk of increase of knock likelihood at medium/high engine load. For mitigating conditions where the engine is prone to knocking, the main adopted control strategies are the mixture enrichment and the spark ignition time retard. At low and moderate engine speeds, knock mitigation is obtained from delaying the spark ignition time advance, thereby penalizing the output torque, the combustion stability, the fuel economy, and leading to an increase in the exhaust temperature. To avoid excessive spark ignition time retard, the Compression Ratio (CR) of the engine is limited, which in turns limits engine efficiency at middle low load and power. Rich mixture is an effective means of both limiting the exhaust temperature at the turbine inlet at high engine speeds and protecting the oxidation catalyst, maximizing engine power but reducing fuel efficiency. The pursued technologies for knock mitigation are cooled EGR, overexpansion cycles (Miller/Atkinson cycles), water injection and TJI (Turbulent Jet Ignition).

II. In January 2017, the EU Commission issued a notice on the new policy regarding the component protection strategy (Auxiliary Emission Strategies AES), as that regarding the fuel enrichment for limiting the Turbine Inlet Temperature (TiT) below the threshold imposed by the turbine thermal limit, mostly at full power condition. These AES have been found to increase dramatically CO emissions since CO cannot be handled by the Three Ways Catalyst (TWC) under rich combustion conditions. According to the perspective of large CO emissions

increase due to fuel enrichment strategy and to the above-mentioned EU Commission notice, the development of S.I. engines operating at stoichiometric conditions in the overall map is strongly recommended.

The water injection is thought to help in fulfilling all these goals, thus contributing towards more efficient engines, because its anti-knock attitude in S.I. engine applications. However, it must be considered that the injection of water changes both the thermodynamics (due to the temperature reduction) and the mixture composition (due to the presence of vaporized water, which acts as an inert specie). To perform a rapid design optimization of the main parameters involved by the application of the water injection, it is necessary to apply reliable CFD methodologies capable of capturing the most important phenomena.

LITERATURE SURVEY

The main positive aspect of the water injection is its strong mixture cooling capability which also increases the engine volumetric efficiency thanks to its high latent heat of vaporization [2, 3].

For clarity's sake, here some scientific works only have been cited. The main topics related to water injection concern the experimental and/or simulated evaluation of the water spray characteristics, depending on the water injector type and installation:

a) Location and orientation.
b) Geometric characteristics.
c) Flow rate.
d) Injection timing.

Lanzafame et al. [4] experimentally and numerically analyzed the effects of both continuous and pulsed water injection in the intake duct at low pressure (10 bar), finding that the water injection operates like an anti-knock additive. Moreover**,** the exhaust gas NOx emissions were cut in half. Brusca et al. [5] applied pulsed water injection, highlighting an increased effect of the anti-knock effect of the water. Boretti [6] presented a comparison between water injection in the intake duct or directly in the cylinder. The injection in the intake duct has a cooling effect on the intake air mass, reducing its density and enhancing engine permeability (volumetric efficiency increase) and power density. The injection directly in the chamber leads to a cooler combustion phase, followed by a lower exhaust temperature. Bhagat et al. [7] performed spray visualization experiments reproducing in the bomb the different injection pressure levels and the air initial temperatures, thus simulating the variable injection phasing during a real engine cycle for a modern turbocharged GDI engine. They demonstrated that DWI at 90 degrees before Top Dead Center TDC resulted in about 8% reduction in peak temperature at the end of the compression stroke compared to without water injection, while a temperature drop of 6% was observed for injection at 60 degrees before TDC. Earlier water injection timings decreased the tendency of liquid film formation (of 53%) maybe because at earlier injection the lower density of the in-cylinder gases allows the spray to preserve its momentum and so to bounce off the surface wall: it results in enhanced vaporization rate and cooling effect. The decrease of the temperature due to water allowed the engine to operate at the MBT (Maximum Brake Torque) spark timing or close to it, while without water the engine would be knock limited under high load-low speed conditions. Finally, if water is introduced late in the compression stroke, it will require less energy to evaporate, leading to a reduced cooling effect on surrounding gases. However, the presence of vapor water could have a positive effect itself on the final peak temperature (reducing it during the compression phase) at TDC due to the increase of specific heat of the combustion chamber gaseous mixture. In [8, 9] the position of the water injector in the intake duct was studied, finding that a closer position to the intake valve reduces the water consumption to less than 50% compared to an upstream position for the same cooling effect. Most of the water injection studies were performed for a Port Water Injection (PWI) solution because it is less costly, and the injector can be easily installed on a pre-existing engine [10]. Some authors [11, 12, 13] worked on a water direct injection system. In general, the injection pressure for PWI applications in literature ranges between 4 bar up to 10 bar [10, 14, 15]. In [16] the primary atomization of water jets at high Reynolds numbers was numerically investigated using a multi-scale Eulerian-Lagrangian approach and measured during some experiments. In [17] the authors have experimentally investigated the spray breakup and atomization process of a Port Injector: the focus has been to investigate a fuel injector, but the experimental injector has been fed by water. Fuel injection pressure and temperature have been varied in the range respectively of 2 to 5 bar and of 25°C to 70°C.

In the current car market, BMW sells the M4-GTS equipped by 3 PWI water injectors, one every two cylinders. They located the water tank in the trunk, with a capacity of 5 liters. The injection pressure is set to 10 bar.

PAPER FOCUS AND FRAMEWORK

In the current research activity, the CFD simulation of non-reacting (PART I paper) and reacting cycles (PART II paper [18]) has been applied to the assessment of water injection application to a S.I. GDI turbocharged engine. The rated power engine operating point has been selected for the present analysis as it is the most demanding in terms of time available for injection, vaporization and water mixing. Both Port Water Injection (PWI) and Direct Water Injection (DWI) architectures have been tested for the same baseline engine configuration and the main results have been checked in terms of evaporation rate, cooling temperature, and efficiency. The main aim of these simulations is to maximize water injection benefits and minimize possible disadvantage, such as primarily oil dilution and incomplete water evaporation: water tank volume and refilling frequency depend on the final value of vaporized water. The water injection systems, both PWI and DWI, have been simulated at full power condition, at the same rated power engine speed by varying: i) the injection pressure; ii) the injection timing (water injection phasing has significant effect on the water evaporation rate and on its impact on walls); iii) the normalized water injected mass on the stoichiometric fuel mass (s parameter, as defined in [2]). The *s parameter* definition is given here for clarity only:

$$s = \frac{m_W}{m_{FUEL_{ST}}} \qquad (1)$$

where m_W is the water mass and m_{FUEL_ST} is the stoichiometric fuel mass according to the estimated trapped mass in the current engine cycle. Moreover, to pursue the target of improving the engine efficiency across the whole engine map, which leads to the reduction of CO_2 emissions and the maintenance of good level of performance, the CR of the baseline engine has been increased. Water injection might allow to use higher CR with limited penalties on performance. The CFD methodology adopted is capable of capturing both the thermodynamic effects of water injection and the chemical kinetics aspects related to the mixture water dilution (see PART II paper [18]) whose prediction is mandatory for addressing the engine design according to different goals: a) complying with new emission directives and limits, b) turbine inlet temperature constraints, c) minimization of the BSFC, d) possibly engine power increase.

The research activity presented in this paper has been split in the following main items, corresponding to as many paragraphs:

1. Literature review.
2. Engine specifications.
3. Description of the simulation environment.
4. 3D-CFD simulations of indirect/direct water injection strategies. In this section PWI and DWI architectures have been analyzed in detail, varying the injection pressure level, the non-dimensional injected water mass and the Start Of Injection (SOI) time. The best solutions for each architecture have been compared for finding out the optimal configuration in terms thermodynamic and fluid-dynamics properties.

The best PWI and DWI solutions have been applied to an improved engine geometry, characterized by an increased CR (from 9.5 to 10.5).

THE ENGINE SPECIFICATIONS

A high-bmep and high-power S.I. GDI turbo-charged engine has been virtually designed at the University of Bologna and slightly modified compared to the previous one [3]. In Figure 1 the engine is visible, in the DWI version in Figure 1a and in the PWI configuration in Figure 1b, respectively. Both configurations have been drawn in order to have the same compression ratio.

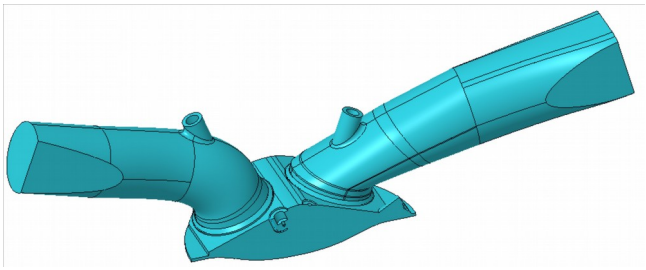

a)

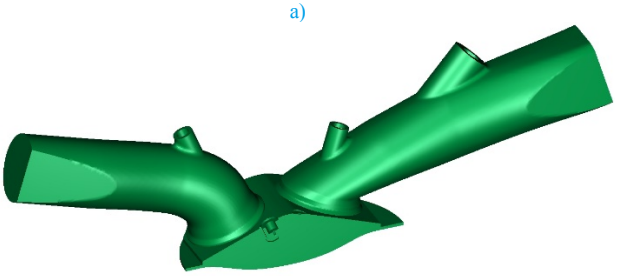

b)

Figure 1. Virtual engine with a) DWI system; b) PWI system

The water injector spray targeting was carefully chosen in both configurations to minimize the wall impingement, especially on the piston periphery, and therefore to promote the water evaporation within the airstream. The injector in the DWI case is mounted on the intake side of the engine head. This helps in the overall drawing of the engine head and it allows larger free spray path between the injector and the cylinder or piston surfaces. Moreover, the water spray beam orientation was set to promote the interaction between the water plumes and the in-cylinder air-flow field, enhancing the water evaporation rate. The spray modelling technique has been validated and results could be found in [19]. The models adopted for both gasoline and water were the same: the model-specific constants were not tuned differently. In PWI case, only the secondary breakup model was activated: the probability distribution function (PDF) was modified on the basis of the validation process. The injector characteristics have been resumed in Table 1. The fuel injector is centrally located with a spray directed towards the spark plug to promote combustion during cat-heating phase. Table 2 resumes the main specifications of the adopted high-bmep engine. The operating point considers the full power condition whose characteristics are listed in Table 3.

Table 1. Gasoline and water injector characteristics

	GASOLINE	DWI	PWI
Number of holes [-]	8.0	5.0	2.0
Injection pressure [bar]	350.0	50.0/150.0	10.0/20.0
Injection temperature [K]	313.0	313.0	313.0
HFR [cm^3/s]	20.0	17.0	17.0
Hole geometric diameter [µm]	188.0	220.0	347.0

Table 2. Main characteristics of the baseline engine

Unit Displacement [cm^3]	471.05
Stroke S [mm]	85.00
Bore D [mm]	84.00
Conrod length [mm]	165.60
Number of valves	4.00
S/D [-]	1.01
Intake valve diameter to bore ratio D_V/D [-]	0.36
Exhaust valve diameter to bore ratio D_V/D [-]	0.33
Compression ratios	9.50:1.00 / 10.50:1.00
Squish Height [mm]	1.10

Table 3. Engine operation point at full power

Engine speed [rpm]	7000.0
Engine load	100.0%
Mixture index (w/o water) [-]	1.0
Boost pressure [bar]	2.7
Max BMEP [bar]	26.6
Inlet valve opening [CA deg. ATDC]	362.0
Inlet valve closing [CA deg. ATDC]	598.0
Exhaust valve opening [CA deg. ATDC]	136.0
Exhaust valve closing [CA deg. ATDC]	376.0

DESCRIPTION OF THE SIMULATION ENVIRONMENT

3D CFD simulations have been performed with the commercial code AVL Fire v. 2020. The boundary and the initial conditions for the CFD simulations at the considered operating point have been derived by running one-dimensional simulations using the open source code OpenWAM. The engine cycle three-dimensional CFD simulations, whose setup is shown in Table 4, were performed following a multi-cycle approach: the presented results refer to the last converged engine cycle. Differencing schemes are second order for mass, momentum and energy, while turbulence is resolved with a second order blended scheme. The solution is converged when the residual error for each equation is below the tolerance threshold of 1e-4. Non-reacting flow simulations have been performed and they have been stopped at TDC of the converged cycle: they are aimed to assess the behavior of the water injection system at the stoichiometric operating condition. Half-geometry domain has been considered because of the symmetry conditions. The computational mesh has 506.000 cells at TDC. The parameter *s* is used to measure the injected water mass per cycle and cylinder, and it is defined as the ratio between the injected water mass and the stoichiometric fuel mass of the given engine operation point. A relative humidity of the ambient air of 40% has been considered.

3D-CFD SIMULATIONS OF INDIRECT/DIRECT WATER INJECTION STRATEGIES – BASELINE ENGINE

For the future emission regulations, it might be necessary to run gasoline engines under stoichiometric conditions. To limit the exhaust gas temperature at full power engine condition without mixture enrichment strategies (i.e. running with stoichiometric mixture), in the present work both PWI and DWI architectures have been deeply analyzed. For current turbocharged S.I. engines, the over fueling strategy, aimed at protecting components such as the turbine, at full load adopts a mixture index λ (properly defined as the air-fuel equivalence ratio: it is the ratio of actual AFR to stoichiometry for a given mixture) variable in the range among λ 0.75 and λ 0.85, where the extra fuel is used to cool the fresh mixture, to limit the TiT value below the threshold value (i.e., from 950 °C to 1050°, depending on turbocharger technology adopted), as imposed by the thermal limits of the turbine material. To highlight the consequences of such a transition from rich to stoichiometric mixture operations, simulations have been performed without water injection at λ=0.75, λ=0.85 and λ=1.0, under non-reacting flow conditions. The latter simulations represent a mandatory reference system for the assessment of the simulation results obtained by applying the water injection strategy under stoichiometric conditions. In the next part of the paper all the analyzed PWI and DWI cases under not-reacting flow conditions will be presented separately for the baseline engine geometry, then the best choices or the most interesting ones for each water injection system will be compared with each other and with the fuel-only case at variable mixture index (λ equal to 0.75, 0.85 and 1.0). Moreover, for the best cases only, the engine configuration in terms of CR has been varied. The most interesting cases have been analyzed under reacting flow conditions in PART II paper [18], next to this one.

Table 4. Main settings for CFD simulations – NON-REACTING FLOW

Start angle	330 CA deg. ATDC

End angle	720 CA deg. ATDC
Turbulence model	K-z-f
Wall heat model	Han-Reitz [20]
Law of the wall	Hybrid wall treatment
Evaporation model	Spalding
Wallfilm evaporation model	Combined
Wallfilm entrainment model	Schadel - Hanratty
Wallfilm splashing model	Kuhnke
Atomization model	Slightly modified version of the model presented in [21]
Breakup model	

All the water injection cases have been run at full power condition, at the same rated power engine speed by varying: i) *the injection pressure*; ii) the *injection timing*; iii) *the parameter s (i.e., the non-dimensional water injected)*.

Fuel-only operations (i.e., without water injection)

The current turbocharged S.I. engines over fueling strategy adopts a mixture index variable in the range among λ 0.75 and λ 0.85, where the extra fuel is used for limiting the TiT value below the threshold limit. Simulations of fuel-only strategies λ 0.75, λ 0.85 represent a mandatory reference system for the assessment of the simulation results obtained by applying the water injection strategy under stoichiometric conditions and they have been reported briefly in this section. They have been also compared to the stoichiometric case, which is the starting condition of the water injection analysis.

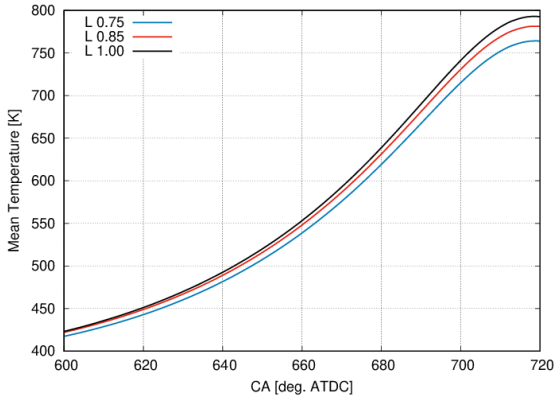

Figure 2. Mean in-cylinder temperature trend during compression stroke – FUEL-ONLY cases

In Figure 2 the mean in-cylinder temperature trend is plotted. As expected, the less is the injected fuel (the leaner the mixture), the higher is the in-cylinder temperature at IVC and at TDC. In particular, at TDC moving from the richest condition to the stoichiometric condition the mixture temperature increases of 29 K (+3.8%).

PWI system

In Table 5 the analyzed cases for PWI systems have been reported. Care has been taken to reduce (not to eliminate) the water spray impingement against the cylinder liner. The injector accommodation and spray pattern configuration have been chosen together with an optimized injection timing

to allow the spray to enter the cylinder. Thanks to the latter, the water spray exploits for the evaporation process more favorable thermodynamic conditions than those it could encounter in the intake manifold and ports. The relative injection pressure was varied in the range between 10 bar and 20 bar. This choice was done to allow the use of the current and well-assessed PFI and UREA technologies, thus reducing costs. A relative injection pressure lower than 10 bar would reduce the flexibility in the injection timing selection and sweep, as already discussed by the authors in [3]. Injection pressures greater than 20 bar are beyond the practical interest because of the associated costs. The SOI and thus the End Of Injection (EOI) timings depend on the injection pressure, the mass of water to be injected per cycle and on the constraint imposed to promote that all the water spray droplets can enter the cylinder before IVC. In the case of PWI strategy, there is a limited flexibility in the choice of the SOI time. Following all these considerations, the SOI/EOI times reported in Table 5 have been fixed.

Table 5. PWI system – Analyzed cases – Stoichiometric conditions – Baseline engine configuration

Parameter s [-]	SOI / EOI [CA deg. ATDC]	Injection pressure [bar]
0.20	293.00 / 390.00	10.00
	363.00 / 460.00	
0.30	293.00 / 433.00	
	320.00 / 460.00	
0.40	277.00 / 460.00	
0.20	318.00 / 390.00	20.00
	393.00 / 465.00	
	413.00 / 485.00	
	433.00 / 505.00	

Table 6. PWI system – Injected fuel and water masses – Stoichiometric conditions

Case (λ 1.00)	Parameter s [-]	Fuel or Water injected mass [mg]
Fuel-only	-	84.00
Water-added	0.20	16.80
	0.30	25.20
	0.40	33.60

In Table 6 the injected masses under stoichiometric conditions for fuel-only case and with variable parameter *s* are summarized. At λ 0.75, the injected fuel mass was 112.8 mg.

The PWI architecture analysis framework is as follows:

a. Injection pressure: 10 bar. The SOI times and the water mass (*s* parameter) have been varied.
b. Injection pressure: 20 bar. The SOI times and the water mass (*s* parameter) have been varied.

c. Comparison between the best solutions of both injection pressures 10 bar and 20 bar. The aim was to find the best WI configuration in terms of injection pressure and mass of water for the analyzed operation condition.

Injection pressure of 10 bar

The present analysis has been subdivided in some parts for clarity seeking:

1. Fluid-dynamics analysis: study of the interaction between the jet spray and the main in-cylinder motions. In this sub-paragraph the effect of the jet spray on the tumble motion formation and on the final level of turbulence close to spark plug at ignition time has been reported.
2. Thermodynamic analysis: temperature at TDC and cooling efficiency. In this sub-paragraph a detailed analysis of the evaporation process and of the spray dynamic has been carried out.
3. Mixture composition close to spark ignition time.

FLUID-DYNAMICS ANALYSIS

In Figures 3 and 4 the tumble ratio and the in-cylinder mean turbulent intensity (evaluated as the ratio between the turbulent fluctuating energy and the mean piston speed) trends have been reported. The tumble ratio trend gives an indication of the formation of a coherent and structured, well centered in the chamber, main vortex, which is the main source of the next turbulence development.

In Figure 3 the tumble trend is visible: increasing the injected mass of water the tumble ratio TR trend moves down with respect to the fuel-only case in dashed line. This trend confirms that there is an interaction between the main intake flow and the jet of the water injector. In the case of PWI architecture, this interaction is not really strong. The spin-up phase (from IVC to about 650 CA deg. ATDC, where the TR curve has its maximum) and the breakdown phase (from 650 CA deg. to TDC) of the tumble motion during the compression stroke are influenced by the water injection, except the case s 0.2 and SOI 293, which has a trend almost overlying the fuel-only case. All the cases have the same low final level of residual TR value at TDC, which denotes a good breakdown phase, typical of a well-structured tumble motion. Looking at this TR trend, it is to expect a very good turbulence level close to spark ignition time, as confirmed by Figures 4a and 4b, where the turbulent intensity trends have been reported in the overall cylinder and in the cylinder domain close to the spark plug location, respectively: case s 0.2 SOI 293 confirms to have the least effect on the intake flow and on the main in-cylinder motion, while the worst case is s 0.3 SOI 320. For what concerns the turbulence level, case s 0.3 SOI 293 is the best solution immediately after the case overlying the fuel-only case (s 0.2 SOI 293).

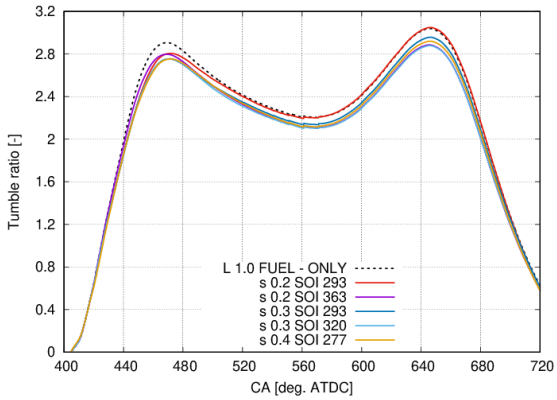

Figure 3. Tumble ratio trend – REFERENCE CASE: λ 1.0 FUEL-ONLY

All the results presented in this section confirm the nature of the intake duct, which has been designed for being “high tumble duct”.

THERMODYNAMIC ANALYSIS

In Figure 5 the temperature difference at TDC with respect to the REFERENCE fuel-only λ 1.0 case has been reported for all the cases of Table 5 at injection pressure of 10 bar, plus the fuel-only cases λ 0.75 and λ 0.85. The stronger drop in temperature obtained by the enrichment strategy compared to that of the stoichiometric operating condition, indicates an adequate minimum target that must be achieved in stoichiometric conditions by exploiting the injection of water.

Looking at Figure 5 it is to highlight that:

a. The temperature level of the richest mixture (λ 0.75) is reached by the smallest mass of injected water with the most advanced SOI strategy (s=0.2 with SOI at 293 ca deg ATDC).
b. For the same mass of water (s), the more advanced is the SOI time, the greater is the water cooling effect.

c. Comparing the different masses of the injected water, the highest cooling effect has been reached for the case s=0.4. It should be noted that this case doubles the injected mass compared to the case s=0.2 but its final temperature difference corresponds to less than double that of the TDC. Moreover, focusing on the increase of the injected water from s=0.2 to s=0.3 (plus 50%), the temperature decrease is 44.5%. Thus, the present calculations highlight that in a PWI system the cooling effect is quite far from being proportional to the increase in the mass of the injected water.

The latter outcome can be explained by analyzing the overall evaporation process during the engine cycle. Figure 6 shows the percentage, with respect to the total mass injected, of the mass of the evaporated water. It should be highlighted that in the present assessment and in the previous ones [2, 3] too, authors have considered successful a configuration or a strategy capable of inducing the evaporation of at least 90% of the injected mass within TDC under non-reacting flow conditions. This criterion is satisfied by all the cases under analysis. It is interesting to focus the attention not only on the maximum evaporated mass at TDC, which decreases with increasing injected mass of water or retarded SOI timing, but also on the evaporation rate trend. The masses of water and fuel remaining liquid in the spray cloud are zero near the TDC: this is related to the fact that in all cases the evaporated mass of water is at least 90% of the injected one, as above commented.

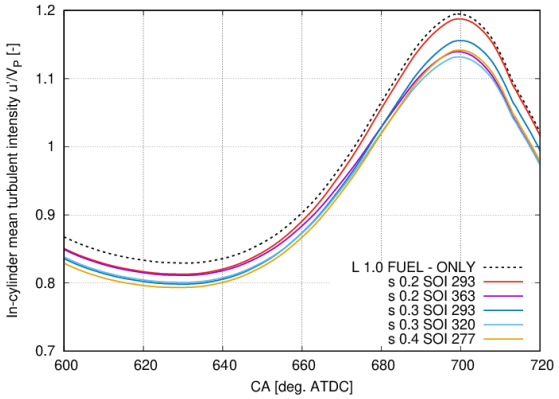

a)

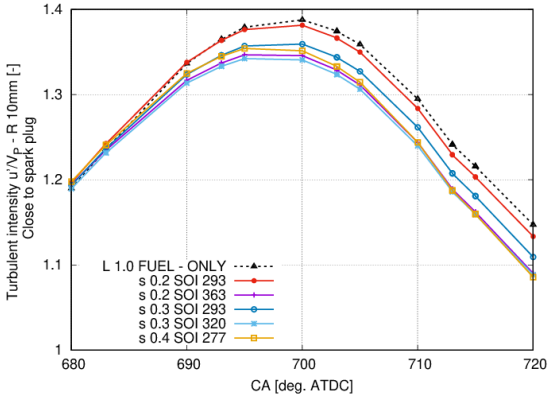

b)

Figure 4. Mean turbulent intensity: (a) mean in-cylinder; (b) close to spark plug inside a radius of 10 mm – REFERENCE CASE: λ 1.0 FUEL-ONLY

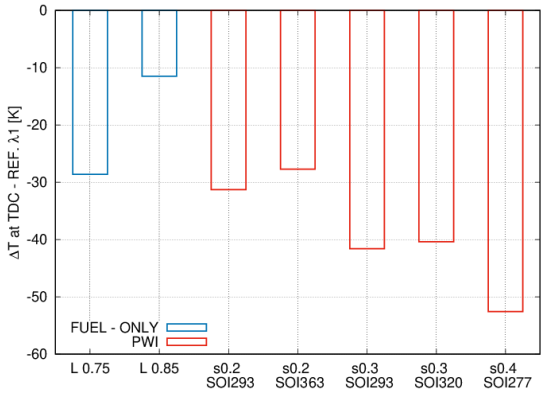

Figure 5. Temperature difference vs REFERENCE CASE λ 1.00 FUEL-ONLY – Injection pressure 10 bar

Finally, Figure 8 shows the percentage of the mass of water that is part of the wallfilm. It should be noted that the lower is the percentage of the evaporated mass, the higher is the wallfilm thickness, being zero the remaining liquid mass in the spray cloud. All these results can be summarized in the concept of the cooling efficiency, introduced by the authors in [22]. The cooling efficiency, $\eta_{COOLING}$, was introduced by the authors for assessing the *quantity of the 'wasted water'*, i.e. the mass of injected water which does not contribute to the cooling of the mixture. In particular, the cooling efficiency $\eta_{COOLING}$ was defined as the ratio of the effective temperature decrease reached at TDC (ΔT_{REAL}) to the ideal (maximum) temperature decrease (ΔT_{IDEAL}) which can be achieved under the assumption of instantaneous (isochoric) vaporization of the whole injected mass of water at SOI conditions, both at the stoichiometric condition:

$$\eta_{COOLING} = \frac{\Delta T_{REAL}}{\Delta T_{IDEAL}} \qquad (2)$$

$$\Delta T_{IDEAL} \cdot c_V \cdot m_{CYL} = m_{H2O} \cdot LHV_{H2O} \qquad (3)$$

Where m_{CYL} and m_{H2O} are respectively in-cylinder mixture and injected water mass, LHV_{H2O} is the water latent heat of vaporization and c_V is the specific heat at constant volume of the mixture.

It is necessary to specify that it was chosen to consider the boundary conditions at SOI for 'weighting' the thermodynamic gap between PWI (intake) and DWI (in cylinder) boundary conditions of pressure and temperature [2, 3]. The cooling efficiency trend is shown in Figure 9, where the cases having the least advanced SOI have been compared because the delayed SOIs, for both s 0.20 and s 0.30, have shown the lowest evaporation rate. Delaying the SOI, time the water evaporation takes place in an environment whose thermodynamic characteristics are less favorable, as visible in Figure 10, where the evaporation rate is depicted for cases s=0.2 SOI 293 and s=0.2 SOI 363 in both intake port and cylinder domains. The evaporation rate in the intake port domain (black line) is not affected by the SOI time, while in the cylinder domain (red line) the retarded SOI induces a slower evaporation process. Given the above, focusing on the least advanced water injection strategies only, the best cooling efficiency is achieved for case s 0.2. Despite this, cases s 0.3 and s 0.4 show to have a cooling temperature greater than that of case s 0.2.

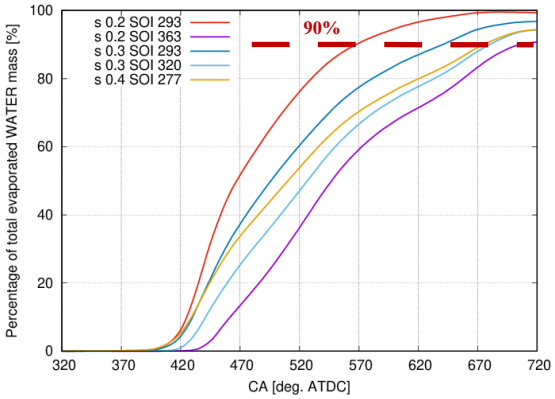

Figure 6. Percentage of evaporated water mass from wallfilm and spray – 10 bar

For choosing the best solution, in Figure 11 the cooling efficiency for variable *s* is depicted versus the temperature reached at TDC: the less is the injected water mass (i.e., the less *s* value), the high is the average temperature reached by the mixture at TDC, the less the is cooling efficiency at TDC. Moving from s=0.3 to s=0.4, the slope of the linking line increases becoming much more vertical than in the first section from s=0.2 to s=0.3, denoting an efficiency drop with respect to the average temperature decrease.

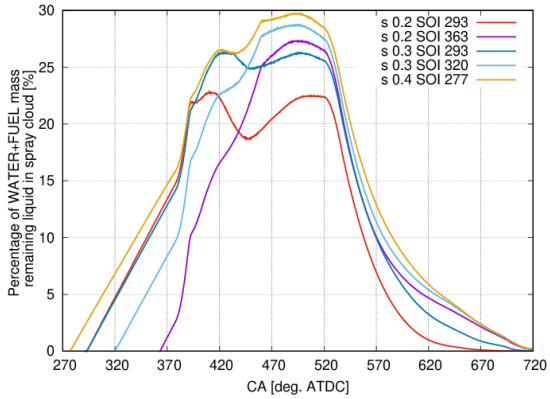

Figure 7. Percentage of WATER+FUEL mass remaining liquid in the spray cloud – 10 bar

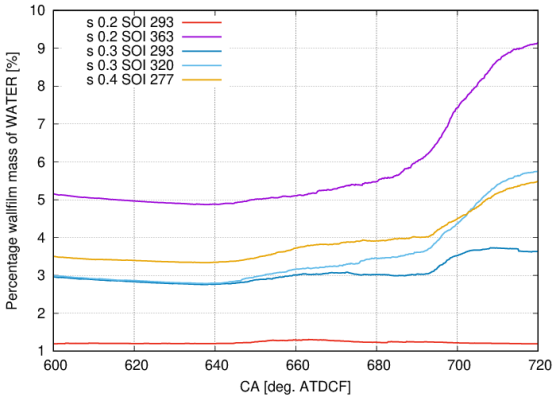

Figure 8. Percentage wallfilm mass of WATER – 10 bar

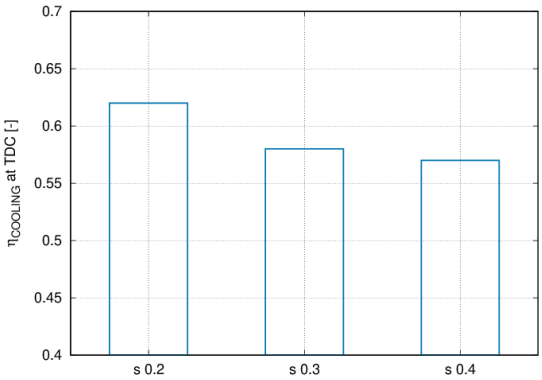

Figure 9. Cooling efficiency at TDC for NON-REACTING flow – 10 bar

Concluding, the best case seems to be s 0.3 SOI 293 CA deg. ATDC at 10 bar, which represents the best trade-off between proper average temperature reduction at TDC and acceptable cooling efficiency.

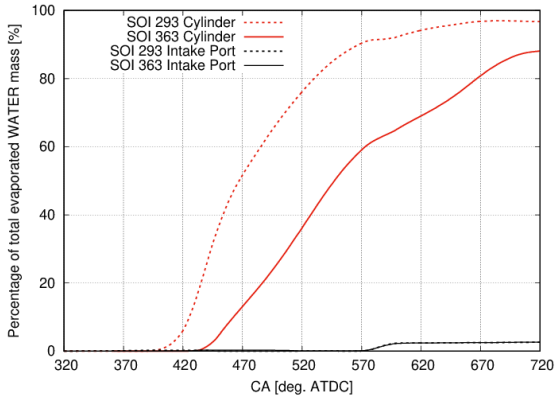

Figure 10. Percentage of evaporated water mass from wallfilm and spray – s= 0.2 – Variable SOI strategy – Intake port and cylinder domains – 10 bar

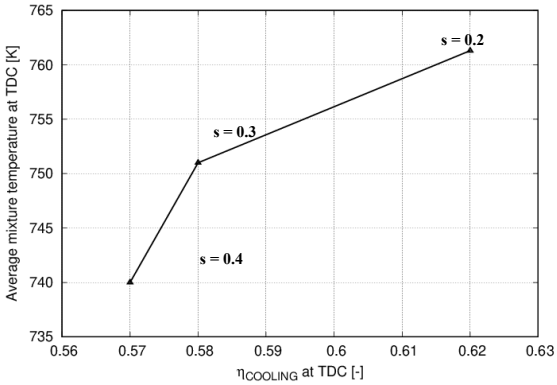

Figure 11. Cooling efficiency at TDC vs Temperature difference with respect to REFERENCE CASE λ 1.00 FUEL-ONLY – 10 bar – Least advanced water injection strategies

MIXTURE COMPOSITION

In this section the main results concerning the mixture composition of the non-reacting mixture under water injection strategy have been reported. In [2, 18] authors have already highlighted that there is a decay of the temperature of the non-reacting mixture with water addition due to not only the heat subtracted to the mixture by the evaporating water but also the decrease of the heat capacity ratio of the mixture (mixture thermodynamic variation), for the same quantity of injected fuel. Another important aspect of the water injection is related to the possible dilution of the mixture, in terms of both absolute value of the mean mixture index compared to the target one and its distribution. The last one can be shortly represented by the standard deviation of the hypothetical Gaussian distribution of the mixture index, which has the target value as mean value, equal to the stoichiometric value in the present analysis. Following this approach, in Figure 12a the mean mixture index trend is shown in the range of possible ignition times, while in Figure 13a the same trend but close to the spark plug location is visible, taking a sphere of analysis having center in the nominal spark plug location and radius of 10 mm. The dashed black line refers to the REFERENCE fuel-only case at λ 1.00. In Figures 12b and 13b the trends of the standard deviation computed with respect to the target value of λ 1.00 have been plotted, mean in the cylinder and close to the spark plug, respectively. The standard deviation may give an indication of the likelihood of the engine, for the examined operation condition, of being prone to detonation: the more is the standard deviation related to mixture quality and turbulence intensity, the more is the probability of having knocking cycles because of the significant non-repeatability of the engine cycles.

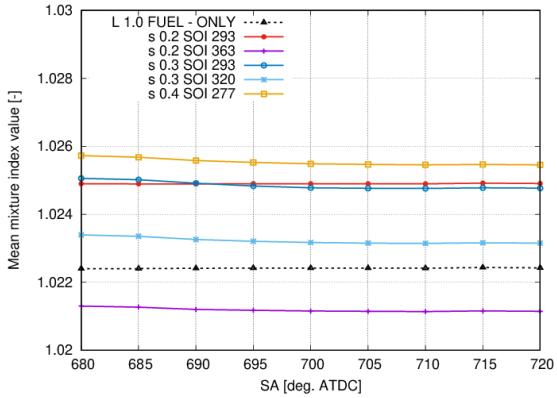

(a)

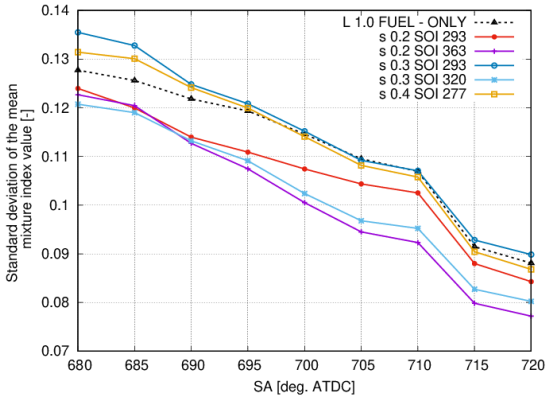

(b)

Figure 12. In cylinder mixture index λ: (a) Mean mixture index; (b) Standard deviation of the mean mixture index

As reported in Table 5, the SOI times and the *s* parameter values were varied, and it is to highlight that:

1. The whole target mixture is a little lean in the cylinder (Figure 12a), while it is stoichiometric around the spark plug at ignition time (Figure 13a). With water addition, there is a kind of dilution effect: the more the SOI of water is delayed, the closer the whole in-cylinder mixture index is to the stoichiometric value (Figure 12a);
2. In the overall cylinder, the least standard deviation is for the case s 0.3 and SOI 363 (Figure 12b), conversely the case s 0.3 SOI 320 has the lowest standard deviation close to the spark plug (Figure 13b).
3. Trying to summarize these results to be a guideline in the next reacting flow analysis [18], it is to highlight that the more the spark advance is delayed, the more the standard deviation reduces: i) up to TDC in the cylinder; ii) up to 705 CA deg. ATDC close to the spark plug location. The mixture index is almost constant in the cylinder, instead the richest fresh mixture is present close to the spark plug in the crank angle range from 695 to 710 CA deg. ATDCF, with a mean value of about 0.95. Note that the closest is the mixture near to the spark plug to 0.95, the fastest is the combustion start phase duration, i.e. the lowest is the angular interval from SA to MFB10 angle (corresponding to 10% of the mass of fuel burnt).

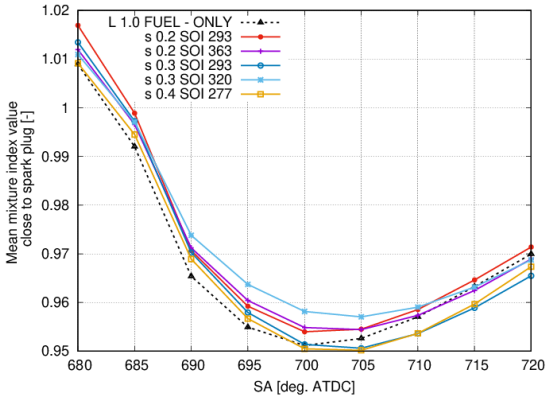

(a)

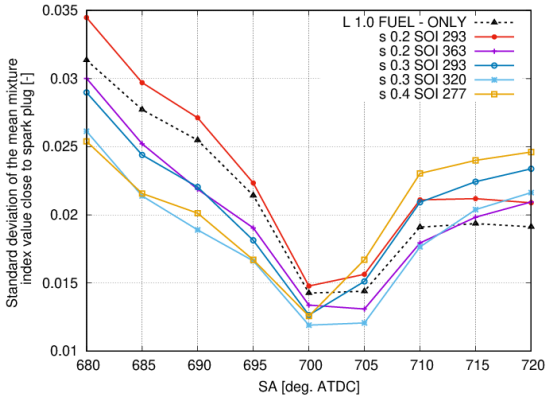

(b)

Figure 13. Close to spark plug mixture index λ: (a) Mean mixture index; (b) Standard deviation of the mean mixture index

Injection pressure 20 bar

For the water injection pressure 20 bar the case s 0.2 only has been tested because it is the case with the highest cooling efficiency, therefore it has been taken as the reference case for the comparison between injection pressures 10 bar and 20 bar. In this case, for the highest injection pressure, only a few results have been reported. The main conclusions drawn for case 10 bar are valid for 20 bar case too.

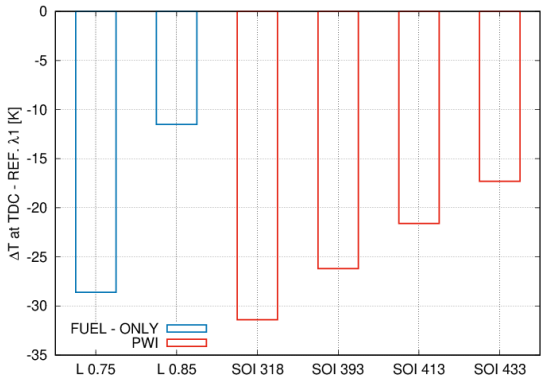

Figure 14. Temperature difference vs REFERENCE CASE λ 1.00 FUEL-ONLY – Injection pressure 20 bar – s 0.20

In this paragraph the SOI time (Table 5) only has been varied for finding the best SOI time. At 20 bar the variation of the SOI time induces a strong temperature difference at TDC (Figure 14) with respect to reference case fuel-only, more than at 10 bar. This is due to the evaporation rate visible in Figure 15: the 90% threshold is reached at SOI 318 only.

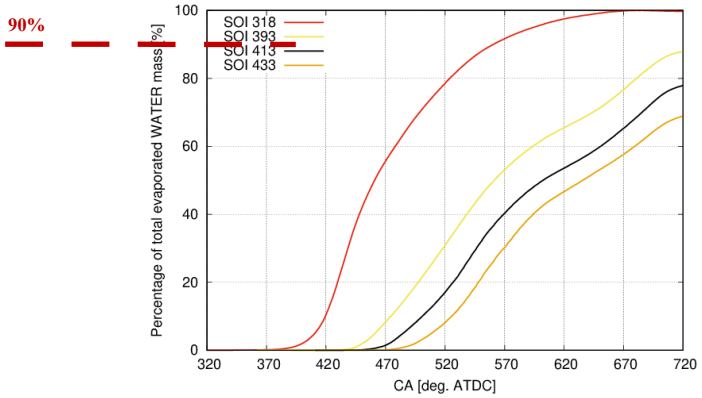

Figure 15. Percentage of evaporated water mass from wallfilm and spray – 20 bar

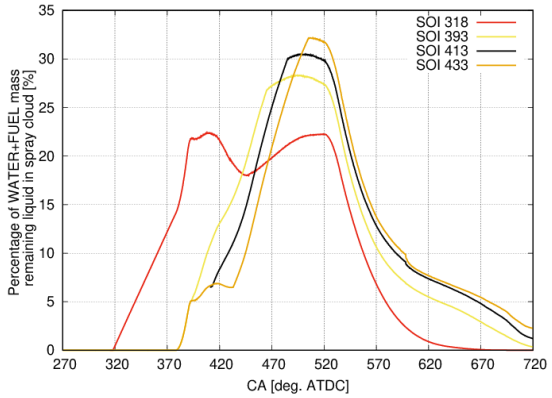

Figure 16. Percentage of WATER+FUEL mass remaining liquid in the spray cloud – 20 bar

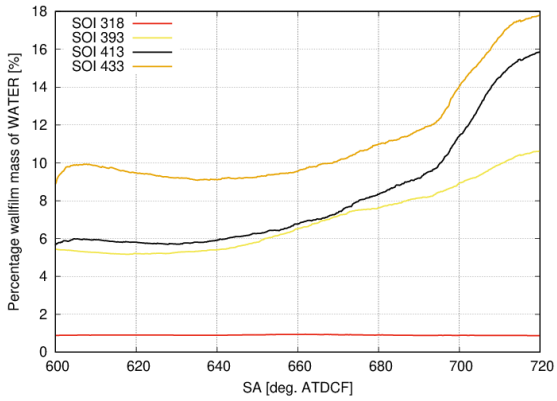

Figure 17. Percentage wallfilm mass of WATER – 10 bar

Case at SOI 318 is the only case where the droplets remain liquid in the spray cloud (Figure 16) and form a thin wallfilm thickness (of the order of 1% of the mass of water injected, as in Figure 17). The case s 0.2 SOI 318 CA deg. ATDC has been then compared to the best case at 10 bar, with the same s parameter, i.e. s 0.2 SOI 293 CA deg. ATDC.

Injection pressures 10 bar vs 20 bar at s 0.2: direct comparison for PWI system

In this section the comparison, for s 0.2, between the case at 10 bar SOI 293 and the case at 20 bar SOI 318 is proposed. In Figures 18, 19 and 20 the comparisons in terms of the temperature difference at TDC computed versus the fuel-only reference case, the mass percentage of water which evaporates in the whole domain and the mass percentage of water that remains liquid in the spray cloud have been reported, respectively.

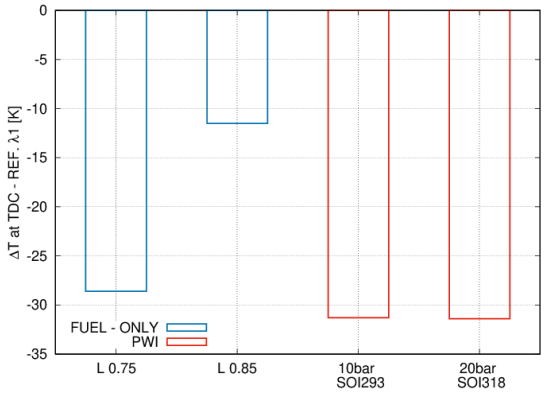

Figure 18. Temperature difference vs REFERENCE CASE λ 1.00 FUEL-ONLY – Injection pressures 10 bar vs 20 bar – s 0.20

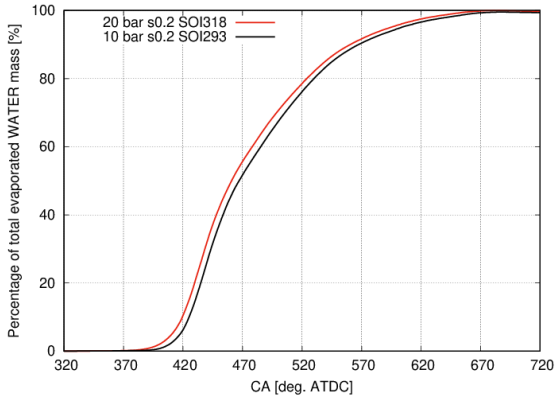

Figure 19. Percentage of evaporated water mass from wallfilm and spray – Injection pressures 10 bar vs 20 bar

It is globally to note that the trends at 10 and 20 bar are almost the same, without notable difference. The only exception is the mass of water in the wallfilm in Figure 21, where it is lowest at 20 bar. Overall, it is to remark that the injection pressure level of 20 bar is more demanding in terms of costs but in authors' opinion its advantages if compared to the 10 bar case are not many.

Finally, in Figure 22 the cooling efficiency has been reported for all cases tested at 10 bar, in their best (the least advanced) SOI configurations, plus the case 20 bar - s 0.2 SOI 318. The 10 and 20 bar cases for the same *s* value have almost the same cooling efficiency, confirming what has just been stated.

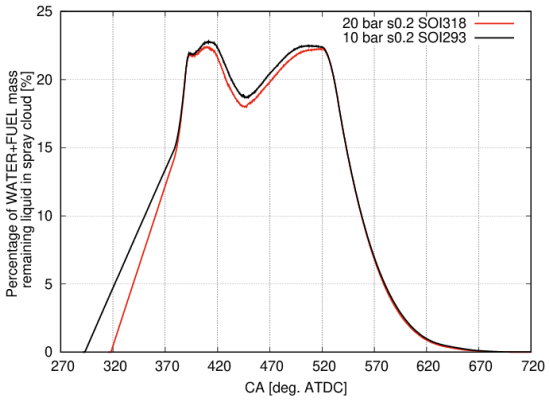

Figure 20. Percentage of WATER+FUEL mass remaining liquid in the spray cloud – Injection pressures 10 bar vs 20 bar

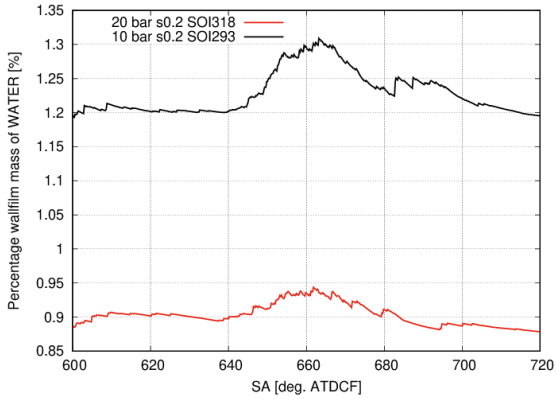

Figure 21. Percentage wallfilm mass of WATER – Injection pressures 10 bar vs 20 bar

Concluding, the best setup for PWI architecture is 10 bar and, limited to the analyzed operation point and engine layout, the best non-dimensional mass of water to inject is s 0.3 at SOI 293 CA deg. ATDC. This configuration has been compared to the best one for DWI case next in the paper.

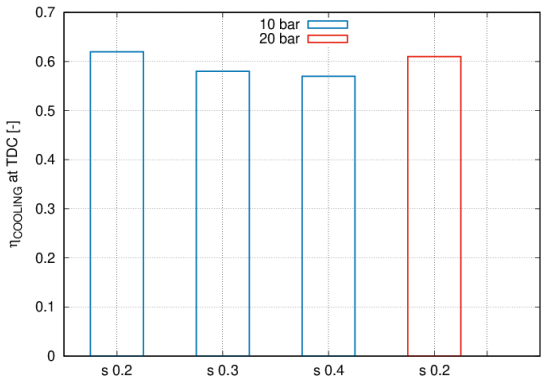

Figure 22. Cooling efficiency at TDC for NON-REACTING flow – Injection pressures 10 bar vs 20 bar

DWI system

In DWI applications there is more flexibility in choosing the SOI or EOI timing. Once fixed the SOI time (or EOI time), the EOI (or SOI) is computed based on the injector flow rate, the injection pressure, and the mass to inject. For resolving this issue independently by the injection pressure level in the injection pressure working range, the authors have developed the concept of 'injection center', not presented here for brevity

seeking. It has been computed the average injection velocity in the chosen pressure range (50, 150 bar) and the mean non-dimensional *s* parameter was set to 0.35 for the further analysis. Starting from these initial conditions, the SOI timing has been optimized to maximize both the cooling effect and the vaporized mass of water. The optimal injection center has been found to be 461 CA deg. ATDC: it has been adopted for the next injection laws at both 50 bar and 150 bar.

For DWI architecture, injection pressures 50 bar and 150 bar have been directly compared.

Injection pressures 50 bar and 150 bar

In Table 7 the analyzed cases for DWI systems have been reported. The injection pressure for DWI strategy has been chosen in the range between 50 bar and 150 bar, i.e. respectively the lowest and the probably highest pressure level for the DWI solution. The lowest injection pressure (i.e. 50 bar) may be the most feasible forecast solution in a near term because of the injection system costs.

In Table 8 the injected masses under stoichiometric conditions for fuel-only case and with variable parameter *s* are summarized.

Table 7. DWI system – Analyzed cases – Stoichiometric conditions – Baseline engine configuration

Parameter s [-]	SOI / EOI [CA deg. ATDC]	Injection pressure [bar]
0.25	409 / 515	50.00
0.35	390 / 533	
0.55	377 / 595	
0.25	429 / 495	150.00
0.35	418 / 506	
0.55	396 / 527	

Table 8. DWI system – Injected fuel and water masses – Stoichiometric conditions

Case	Parameter s [-]	Injected mass [mg]
Fuel-only	84.00	
Water-added	0.25	21.00
	0.35	29.40
	0.55	46.20

In this section a direct comparison between injection pressures 50 bar and 150 bar has been performed.

FLUID-DYNAMICS ANALYSIS

The aim of this paragraph is to understand the effect of the DWI injection on the structured mean in-cylinder motion and if there is a strong influence of the water jet on the final level of turbulence close to spark timing. The TR trend has been reported in Figure 23. The black line is for the stoichiometric fuel-only reference case: this TR trend is always above all other trends. There is a more dynamic effect of the injected mass of water than of the injection pressure levels: the more is the injected mass of water, the lower is the TR. The same trend is visible for the mean in-cylinder turbulent intensity during the compression stroke (Figure 24).

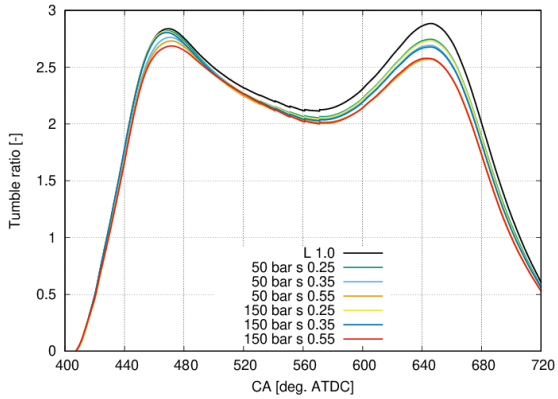

Figure 23. Tumble ratio - Injection pressures 50 bar and 150 bar

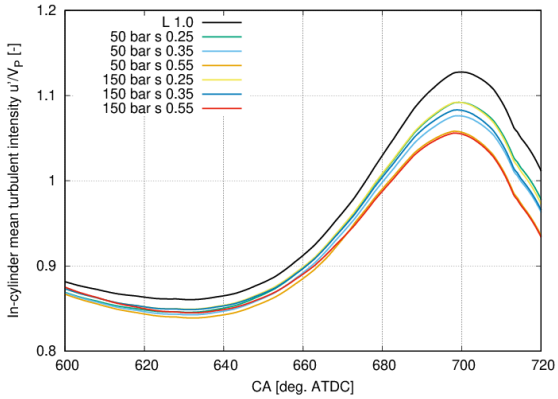

Figure 24. Mean turbulent intensity trend during compression stroke - Injection pressures 50 bar and 150 bar

Figure 25 shows the turbulent intensity behavior close to spark plug: first, there is a shift of the curves with water addition if compared to the fuel-only case. The latter has a peak around 700 CA deg., while the water-cases have a peak from 690 to 700 CA deg. ATDC, but more pronounced. The increase of turbulence close to the spark plug with water addition is around 7%. This latter result demonstrates how the DWI injection interacts via the jet of the water injector with the main intake flow. In the case of PWI architecture, this interaction is not strong. In the DWI case, this interaction enhances the turbulence generation process and then the turbulence increase.

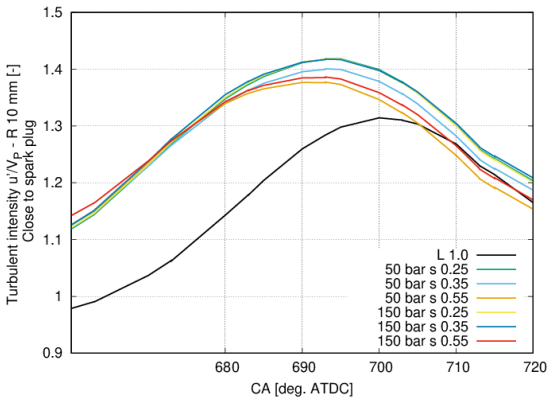

Figure 25. Mean turbulent intensity trend close to spark plug - Injection pressures 50 bar and 150 bar

THERMODYNAMIC ANALYSIS

In Figure 26 the temperature difference at TDC with respect to the REFERENCE case λ 1.0 is visible, for both fuel-only case and with water addition. The final temperature difference (ΔT) reached by the richest mixture (λ 0.75) represents in the analysis the MINIMUM level that must be reached by injecting the water. The analysis shows that the case with the lowest amount of water injected (s 0.25) and at 50 bar already provides a mixture cooling ΔT at TDC which is greater than the best one (28 K) provided by the most favorable reference case operated with fuel enrichment strategy only. Focusing on the final cooling effect only, the best solution would seem to be 150 bar and s 0.55. Nevertheless, it is to note that for the

same mass of injected water (*s* fixed), the higher is the injection pressure, the higher is the temperature difference with respect to the stoichiometric case, which represents a performance evaluation parameter. Moreover, seeking for efficiency evaluation, in Figure 27 the cases running at s 0.35 have been compared for both injection pressures in terms of cooling efficiency: the higher is the injection pressure, the higher is the cooling efficiency.

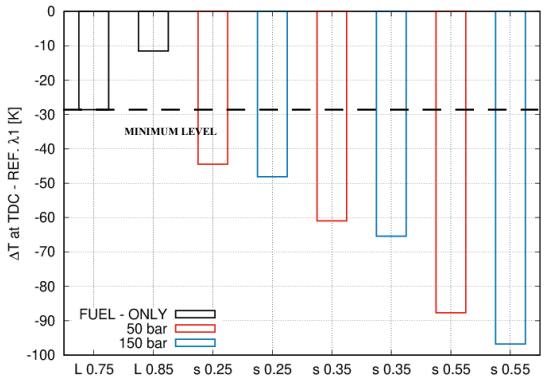

Figure 26. Temperature difference at TDC vs REFERENCE CASE λ 1.00 – Injection pressures 50 bar and 150 bar

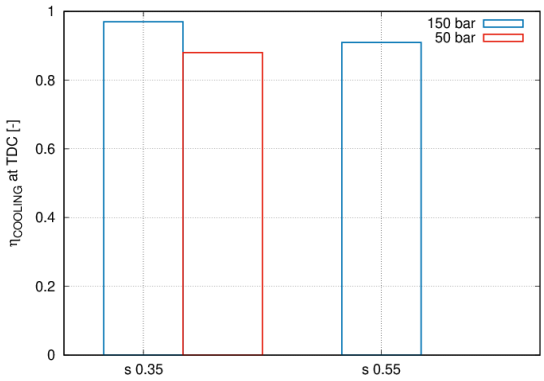

Figure 27. Cooling efficiency at TDC – Injection pressures 50 bar and 150 bar

For understanding the reasons for what has been just illustrated, it is necessary to consider the evaporation process and the spray dynamics. In Figure 28, where the percentage of evaporated mass is plotted in the whole domain, it is to note that at 50 bar the evaporation process is slower than at 150 bar: it starts before but with a less slope. Case at s 0.55 is critical for both injection pressures but 50 bar case is the most critical: the percentage of mass totally evaporated is less than in s 0.25 and s 0.35 cases. Indeed, at s 0.55 and 50 bar a small number of droplets in the spray is still liquid at TDC, as visible in Figure 29. In Figure 30, s 0.25/0.35 -150 bar cases show to have the lowest wallfilm mass, while wallfilm mass at s 0.55 is more than double that of the other cases with the same injection pressure. Moreover, the less is the injection pressure, the more is the wallfilm mass.

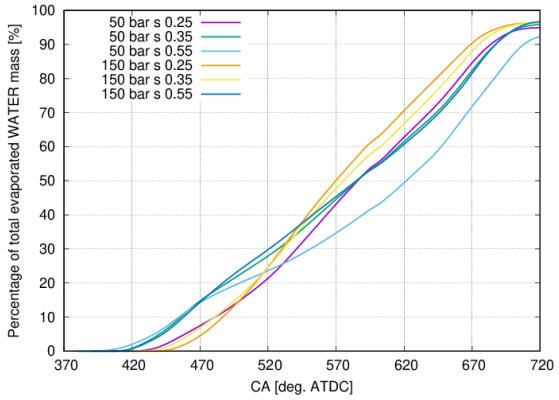

Figure 28. Percentage of evaporated water mass from wallfilm and spray – Injection pressures 50 bar and 150 bar

Pursuing the maximum fuel efficiency, the best choice is 150 bar. Instead, considering the costs, the best solution would be 50 bar. It was then chosen to analyze, also under reacting conditions [18], the cases s 0.35 at 50 bar and 150 bar, which represent the best trade-off between performance and

costs. Moreover, it is interesting to note that the case s 0.55 at 150 bar has the highest cooling effect (Figure 26) but a cooling efficiency lower than the same case at s 0.35 (Figure 27): this case too has been analyzed in detail under reacting conditions [18].

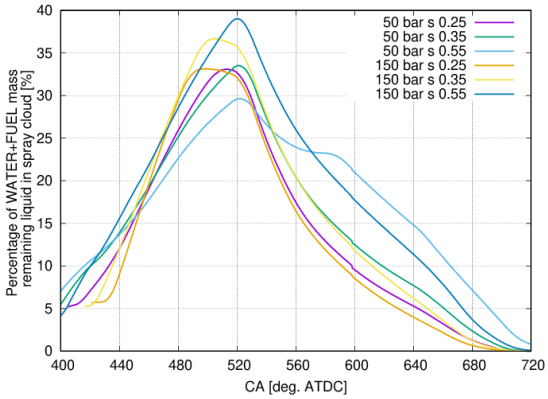

Figure 29. Percentage of WATER+FUEL mass remaining liquid in the spray cloud – Injection pressures 50 bar and 150 bar – WHOLE DOMAIN

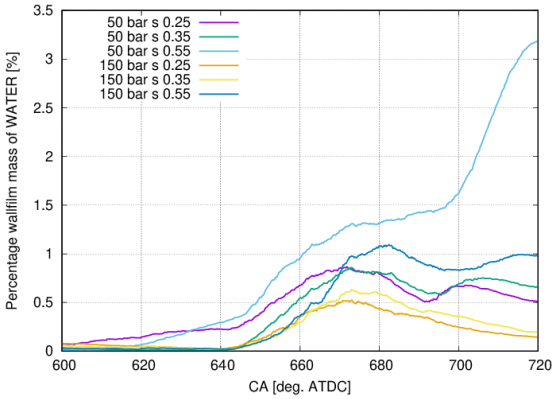

Figure 30. Percentage wallfilm mass of WATER - Injection pressures 50 bar and 150 bar

MIXTURE COMPOSITION

This analysis is focused on the definition of the effect of both the mass of water and the injection pressure on the mixture index distribution in the overall chamber or close to spark plug location. In Figure 31 the mean in-cylinder mixture index (Figure 31a) and its standard deviation (Figure 31b) have been reported, while in Figure 32 the same trends but close the spark plug location are visible.

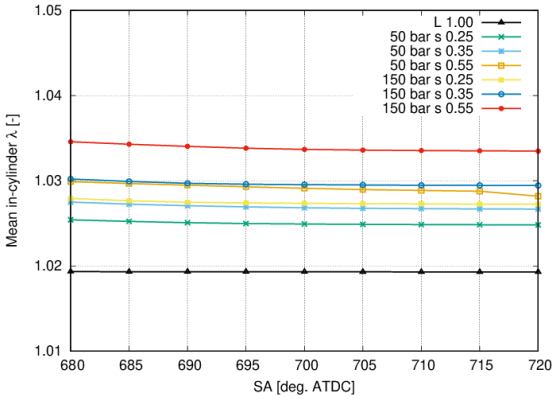

a)

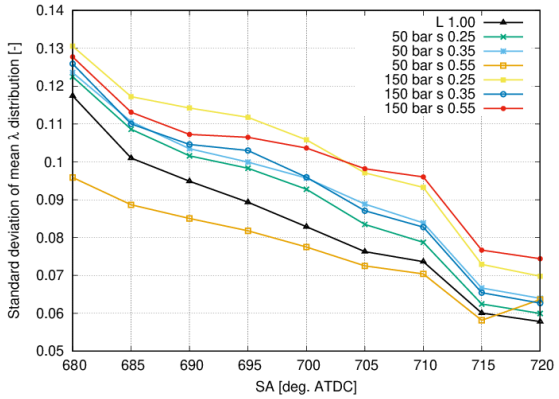

b)

Figure 31. In cylinder mixture index λ: (a) Mean mixture index; (b) Standard deviation of the mean mixture index

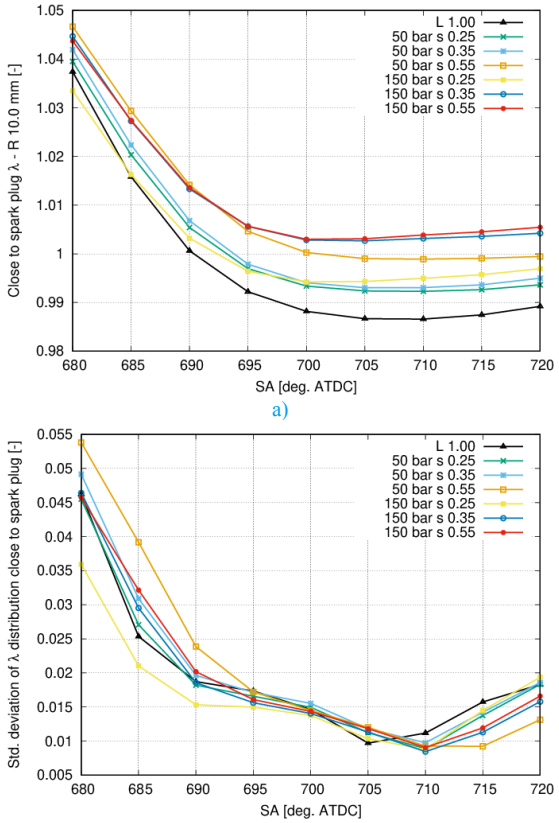

a)

b)

Figure 32. Close to spark plug mixture index λ: (a) Mean mixture index; (b) Standard deviation of the mean mixture index

Adding water, the mean mixture index is leaner than in fuel-only case. Increasing the mass of injected water, the mixture gets leaner, and the same if increasing the injection pressure. Then, the leanest case is 150 bar - s 0.55. The trend is the same close to the spark plug. In the cylinder, the less standard deviation, so the most repeatable distribution, is for fuel-only case, together with case 50 bar s=0.55. Anyway, all analyzed cases have standard deviation values close to each other, both in the overall cylinder and close to the spark plug location.

In the PART II paper [18] it will be shown the importance of the amount of vaporized water for determining the laminar flame speed value: it is lowered by the presence of important percentage of water mass, which acts as a diluter. In the combustion initial phase, which lasts from SA timing to the angle corresponding to the 10% of fuel burnt (MFB 10 angle), a less percentage mass of water should enhance the laminar flame speed, leading to most repeatable combustion cycles.

Comparison between PWI and DWI best configurations compared to rich mixture strategies

As already widely discussed, the performance of the water injection must be analyzed under several aspects. In this paragraph a comparison between the best solutions, i.e. those highlighted in the previous paragraphs, has been performed:

1. DWI:
    a. 150 bar: s 0.35, s 0.55;
    b. 50 bar: s 0.35
2. PWI:
    a. 10 bar: s 0.30.

Previously in the paper, a deep analysis of the single cases in terms of fluid-dynamics and thermodynamic behavior, plus mixture formation aspects, has been reported. From this analysis, some macroscopic evaluation indexes emerge: a) temperature difference with respect to the reference fuel-only stoichiometric case at TDC; b) cooling efficiency at TDC; c) evaporation rate; d) standard deviation of the mixture index close to the spark plug, which is a measure of its distribution; e) tumble ratio TR and mean in-cylinder turbulent intensity trends. The following analyses will be focused on these parameters only for brevity seeking.

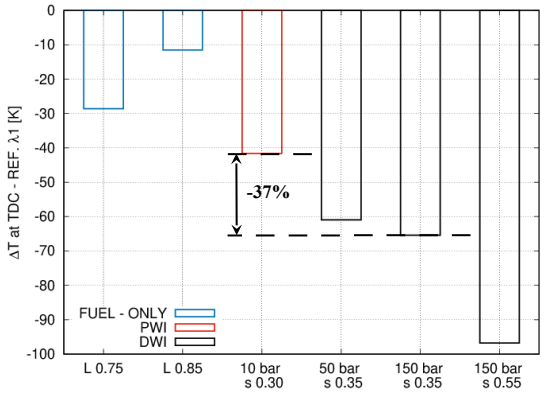

Figure 33. Temperature difference at TDC vs REFERENCE CASE λ 1.00

In Figure 33 the temperature difference with respect to the reference fuel-only stoichiometric case has been reported. The PWI solution provides the weakest cooling effect on the final temperature at TDC, but it is to remember that it has also the lowest amount of injected mass of water. The best DWI solution is achieved for s 0.55 and an injection pressure of 150 bar, as already mentioned before. The PWI system operated at the injection pressure of 10 bar and with s= 0.3 results in a final mixture temperature drop at TDC which is 24 K (- 37.0%) lower than that provided by the DWI system at the injection pressure of 150 bar and with s=0.35.

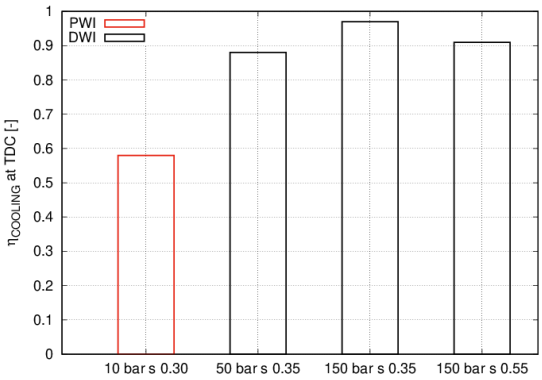

Figure 34. Cooling efficiency at TDC

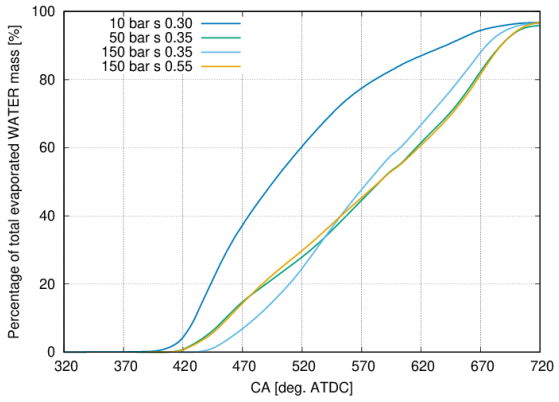

a)

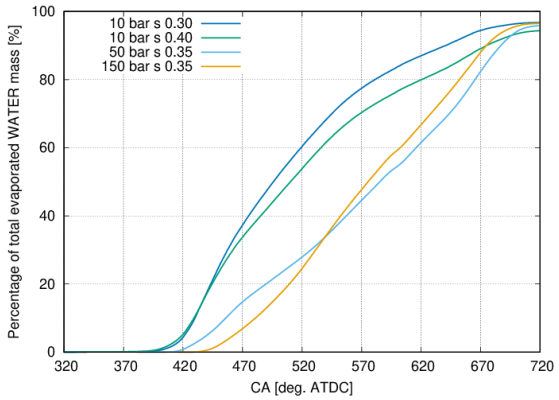

b)

Figure 35. Percentage of evaporated water mass from wallfilm and spray: a) comparison for s=0.30, s=0.35, s=0.55; b) comparison for s=0.30, s=0.35 and s=0.4 – PWI and DWI strategies

Figure 34 compares the cooling efficiency between the different solutions. The most efficient system is DWI – 150 bar – s 0.35, while the less efficient is PWI system. The latter exhibits a cooling efficiency lower than 60% meaning that only a part of the injected water is effective in the mixture cooling. Figure 35a shows that the evolution of the percentage mass of water totally evaporated is different between PWI and DWI systems. It is interesting to note that the final value of the mass of water which is evaporated is almost the same, but in PWI case the process is faster: the liquid finds the best thermodynamic conditions for its evaporation.

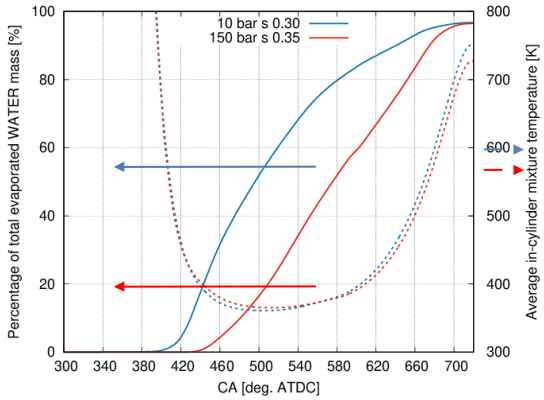

Figure 36. Percentage of total evaporated water mass and in-cylinder average temperature for PWI (10 bar s=0.30 in red line) and DWI (150 bar s=0.35 in blue line) cases

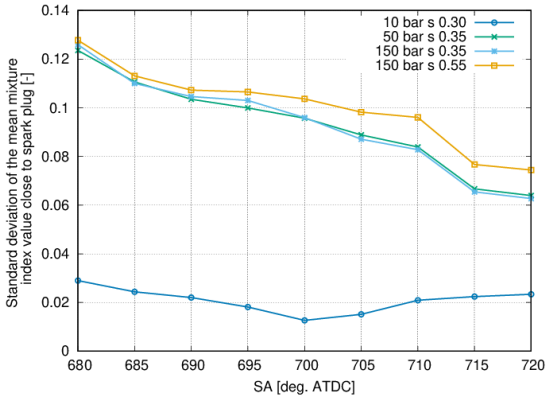

Figure 37. Standard deviation of the mean mixture index close to spark plug – R 10 mm

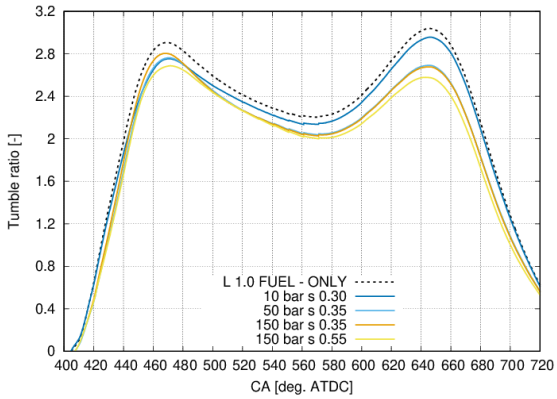

Figure 38. Tumble ratio trend

For explaining this last result, first of all it is necessary to point out that, despite the PWI case at 10 bar has a lower mass of water injected (s=0.30) than the DWI case at 150 bar s=0.35, this is not the main reason: as visible in Figure 35b, the 90% of totally evaporated mass of water is reached at the same angle for PWI 10 bar s=0.4 and DWI 150 bar s=0.35. The reason of the faster evaporation rate for the PWI system must be searched in the different thermodynamic conditions at water SOI time. In Figure 36 the percentage of totally evaporated mass of water and the average in-cylinder temperature are depicted for both PWI (10 bar s=0.30) and DWI (150 bar s=0.35) cases: it is to note that the advanced timing of SOI for the PWI system promotes the evaporation because the latter takes place at higher temperatures than those typical of the DWI case (the in-cylinder temperature difference at the two different start of evaporation times is about 400K). It is to recall here that the water SOI timing for the DWI case must be delayed some degrees after 360 CA deg. ATDC in order to avoid the liquid impingement on the piston surface. Moreover, the delayed timing of SOI for the DWI strategy promotes the achievement of the evaporation target (90%) within TDC, as commented by the authors in [2, 3].

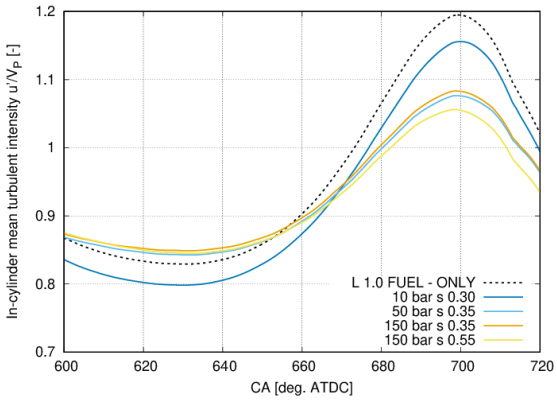

Figure 39. Mean turbulent intensity trend during compression stroke

Moving to the analysis of the mixture composition, the standard deviation of the hypothetical gaussian distribution of the mean in-cylinder mixture index close to the spark plug is shown in Figure 37: it is lower for PWI case than for DWI case because there is less interference between the liquid jet and the mean in-cylinder flow field, as highlighted by the TR trend in Figures 38. The TR trend for the PWI case is the closest to the fuel-only case. This implies a maximum level of turbulence (Figure 39) very close to the fuel-only case for the PWI strategy. Therefore, it is reasonable to expect a less cyclic variability for PWI solutions. These results, together with the less cost, induce to consider the PWI system the most promising solution in the very near future for automotive applications.

3D-CFD SIMULATIONS OF INDIRECT/ DIRECT WATER INJECTION STRATEGIES – NEW ENGINE GEOMETRY

Given the cooling effects of water outlined above, the idea has been to move the engine design towards more 'efficient' configurations. Therefore, the baseline engine has been modified in terms of geometric compression ratio for both PWI and DWI architectures in order to assess the different effects of the injection strategy. The analyzed cases have been DWI s 0.35 150 bar and PWI s 0.30 10 bar.

Compression ratio 9.5 vs 10.5 – PWI vs DWI architectures

The baseline engine configuration was varied in terms of CR. A value of CR higher than 10.5 was not feasible because of the intrinsic drawing limits in the present baseline geometry of the combustion system. The simulations have been performed keeping constant the trapped air mass and thus the fuel mass, under stoichiometric conditions. Thus, this choice brings to an effective increase of the output power because of the thermodynamic efficiency rise linked to the CR increment. Thus, to have the same rated power of the baseline engine, it would be necessary to reduce the fuel consumption and so the trapped mass, together with the reduction of the boost pressure of the turbocharger. The last would be another advantage in terms of losses reduction.

The analyzed cases have been DWI s 0.35 150 bar, referred to as DWI in the following, and PWI s 0.30 10 bar, referred to as PWI in the following, both applied to the engines having CR 9.5 (baseline engine configuration) and 10.5.

In Figure 40 the temperature difference using as REFERENCE the temperature of the FUEL-ONLY CASE at stoichiometric condition (i.e, λ 1.0) at TDC is shown. The higher values of the mass-averaged in-cylinder temperature difference indicate a better charge cooling, while lower values denote possible knocking issues and NOx emission increase, as well as the risk to overcome the TiT threshold. Moving from λ 0.75 to λ 1.00 there is a decay of the temperature difference, due to the reduction of the injected fuel and the increase of the heat capacity ratio of the mixture. The DWI water injection for baseline engine (CR 9.5) results in a remarkable temperature difference versus the reference case λ 0.75. Increasing the CR from 9.5 to 10.5, there is a temperature difference reduction, but the final temperature difference is still much above the reference value at λ 0.75 (blue dashed line). In case of PWI architecture, moving from CR 9.5 to CR 10.5 the temperature difference falls below the reference level of λ 0.75 but for very little, thus remaining still of interest for the future analyses. From above appears the greater potential of the DWI system than the PWI system in terms of water consumption, despite the expected larger cost of the solution (high-pressure injector, high-pressure pump with technology challenge in reliability) and other concerns like those relying the water injector reliability and the lubricant contamination. This temperature evaluation, compared to the stoichiometric case without water injection, is then a measure of the net performance of the water injection. The temperature difference with respect to the reference case increases with the injected water mass but not linearly.

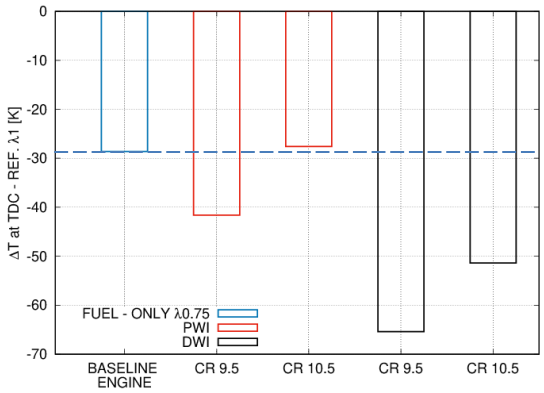

Figure 40. Temperature difference for FUEL-ONLY NON-REACTING FLOW - Mixture index moved from 0.75 to 1.00, w/ and w/o injected water – REFERENCE CASE λ 1.0 at TDC

The evaporation rate in mass percentage is visible in Figure 41: changing the CR, the evaporation process is very similar for each type of architecture and also for the final value in the PWI case. For the DWI architecture, the increase of the CR induces an increment of the final level of the evaporated mass of water, which increases the cooling efficiency too. It is to observe that this increase of the mass of water vapor for CR 10.5 in the DWI system could lead to a slowdown of the combustion process, which adds up to that related to the CR increase from a geometric point of view, due to the worsening of the surface-to-volume ratio (S/V) of the combustion chamber.

Finally, in Figure 42 the mean in-cylinder turbulent intensity trend is depicted for the four cases in analysis. The CR increase leads to a turbulent intensity increase due to more efficient compression of the main tumble vortex during spin-up and breakdown phases. As already noticed, the PWI architecture has turbulent intensity values greater than DWI system at equal CR. Therefore, increasing the CR there is a worsening of the S/V ratio of the combustion chamber (notable during the combustion process) but there is also an increase in the level of turbulence: the laminar flame speed, among others, also depends on them. In the reacting flows analysis [18], it will be necessary to evaluate the effective influence on the laminar flame speed. The CR increase has been obtained adopting the same piston as the case at CR 9.5: these results suggested the necessity to review at least the piston design. It is well known that increasing the CR there is a consequent turbulence reduction, which could be very penalizing in such an engine.

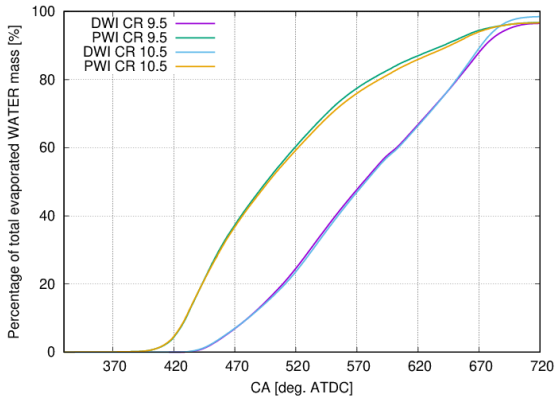

Figure 41. Percentage of evaporated water mass from wallfilm and spray

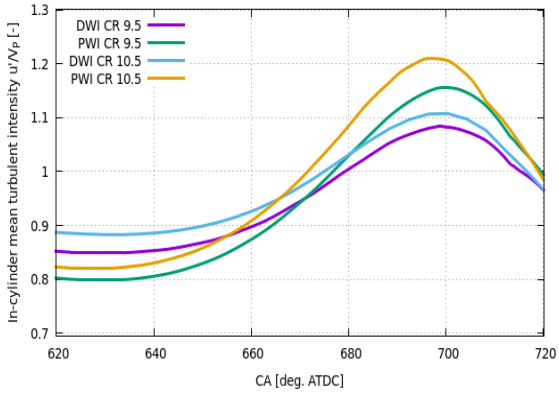

Figure 42. Mean turbulent intensity trend during compression stroke

Conclusions

A methodology for the CFD simulation of non-reacting (PART I paper) and reacting cycles (PART II paper [18]) of S.I. GDI turbocharged engine under water injection operation has been pursued. Both Port Water Injection (PWI) and Direct Water Injection (DWI) architectures have been tested for the same baseline engine configuration and the main results have been checked in terms of evaporation rate, cooling temperature, and efficiency. The main aim of these simulations was to maximize water injection benefits and minimize possible disadvantage, such as primarily oil dilution, related to the presence of liquid water in the chamber at TDC, and incomplete water evaporation. The water injection cases, both PWI and DWI, have been run at full power condition, at the same rated power engine speed by varying: i) the injection pressure; ii) the injection timing; iii) the mass of water injected normalized on the mass of stoichiometric fuel (*s* parameter). Moreover, for pursuing the target of improving the engine efficiency over the whole engine map for CO_2 emission reduction and maintaining a good performance level, the compression ratio CR has been increased. Water injection might allow to use higher CR with limited penalties on performance. The pursued methodology has demonstrated of being capable to capture not only the thermodynamic effects of water injection but also the mixture water dilution.

A deep analysis of the single cases in terms of fluid-dynamic and thermodynamic behavior has been reported. The main results only have been summarized here:

1. PWI architecture: the whole trends at 10 and 20 bar are almost the same, without notable difference. Considering that the injection pressure level of 20 bar is more cost demanding, in authors' opinion its advantages if compared to the case at 10 bar are not many. Thus, for PWI architecture the best solution is s 0.3 at 10 bar, SOI 293 CA deg. ATDC.
2. DWI architecture:
    a. The injection pressure levels have been varied in the range 50 and 150 bar;
    b. Results obtained running the simulations at 50 bar and 150 bar have been compared, changing the mass of injected water. Pursuing the maximum fuel efficiency, the best choice is 150 bar. Instead, considering the costs, the best solution would be 50 bar. It was then chosen to analyze under reacting conditions the cases s=0.35 at 50 bar and 150 bar.
3. PWI vs DWI architecture: the most efficient system is DWI – 150 bar – s 0.35, while the less efficient is PWI system: the latter means that only a part of the injected water is useful in the mixture cooling. The PWI turbulent intensity trend is the closest to the fuel-only case.
4. CR increase: the evaporation process is very similar for each architecture type and also in the final value in case of PWI system. For DWI architecture, the CR increase induces an increment of the final level of evaporated mass of water, which increases the cooling efficiency too. The CR increase leads to a turbulent intensity enhancement due to the more efficient compression phase of the main tumble vortex during both the spin-up and the breakdown phases. The PWI architecture has turbulent intensity values greater than those of the DWI system at the same CR.

From these analyses some interesting configurations, for both PWI and DWI architectures, have been collected for being analyzed under reacting flow conditions in the PART II paper [18].

References

1. Cordier, M., Lecompte, M., Malbec, L.-M., Reveille, B. et al., "Water Injection to Improve Direct Injection Spark Ignition Engine Efficiency," SAE Technical Paper 2019-01-1139, 2019, doi:10.4271/2019-01-1139.
2. Stefania Falfari, Gian Marco Bianchi, Giulio Cazzoli, Claudio Forte, Sergio Negro, "Basics on Water Injection Process for Gasoline Engines", Energy Procedia (2018) pp. 50-57 DOI information: 10.1016/j.egypro.2018.08.018.
3. Falfari, S., Bianchi, G.M., Cazzoli, G., Ricci, M. et al., "Water Injection Applicability to Gasoline Engines: Thermodynamic Analysis," SAE Technical Paper 2019-01-0266, 2019, doi:10.4271/2019-01-0266.
4. Lanzafame, R., "Water Injection Effects In A Single-Cylinder CFR Engine," SAE Technical Paper 1999-01-0568, 1999, https://doi.org/10.4271/1999-01-0568.
5. Brusca, S. and Lanzafame, R., "Water Injection in IC - SI Engines to Control Detonation and to Reduce Pollutant Emissions," SAE Technical Paper 2003-01-1912, 2003, https://doi.org/10.4271/2003-01-1912.
6. Boretti, A., "Water injection in directly injected turbocharged spark ignition engines", Applied Thermal Engineering, 52(1):62 - 68, 2013, https://doi.org/10.1016/j.applthermaleng.2012.11.016.
7. Bhagat, M., Cung, K., Johnson, J., Lee, S. et al., "Experimental and Numerical Study of Water Spray Injection at Engine-Relevant Conditions," SAE Technical Paper 2013-01-0250, 2013, https://doi.org/10.4271/2013-01-0250.
8. D'Adamo, A., Berni, F., Breda, S., Lugli, M. et al., "A Numerical Investigation on the Potentials of Water Injection as a Fuel Efficiency Enhancer in Highly Downsized GDI Engines," SAE Technical Paper 2015-01-0393, 2015, doi:10.4271/2015-01-0393.
9. Pauer, T., Frohnmaier, M., Walther, J., Schenk, P. et al., "Optimization of Gasoline Engines by Water Injection," in: 37th International Vienna Motor Symposium, 2016.
10. Cavina, N., Rojo, N., Businaro, A., Brusa, A. et al., "Investigation of Water Injection Effects on Combustion Characteristics of a GDI TC Engine," SAE Int. J. Engines 10(4):2209-2218, 2017.

11. Jaeheun Kim, Hyunwook Park, Choongsik Bae, Myungsik Choi, Younghong Kwak “Effects of water direct injection on the torque enhancement and fuel consumption reduction of a gasoline engine under high-load conditions”, International Journal of Engine Research, Volume: 17 issue: 7, page(s): 795-808, https://doi.org/10.1177/1468087415613221.
12. Hoppe, F., Thewes, M., Baumgarten, H. Dohmen, J., “Water injection for gasoline engines: Potentials, challenges, and solutions”, International Journal of Engine Research, 2015, Volume: 17 issue: 1, page(s): 86-96, https://doi.org/10.1177/1468087415599867.
13. Hoppe, F., Thewes, M., Seibel, J., Balazs, A. et al., "Evaluation of the Potential of Water Injection for Gasoline Engines," SAE Int. J. Engines 10(5):2500-2512, 2017.
14. Busuttil, D., Farrugia, M., “Experimental investigation on the effect of injecting water to the air to fuel mixture in a spark ignition engine”, March 2015MM Science Journal, 2015(01):585-590, doi: 10.17973/MMSJ.2015_03_201510.
15. Worm, J., Naber, J., Duncan, J., Barros, S. et al., "Water Injection as an Enabler for Increased Efficiency at High-Load in a Direct Injected, Boosted, SI Engine," SAE Int. J. Engines 10(3):951-958, 2017, https://doi.org/10.4271/2017-01-0663.
16. Mahdi Saeedipoura, Simon Schneiderbauerab, Gregor Plohl, Günter Brenn, Stefan Pirkera. Multiscale simulations and experiments on water jet atomization. International Journal of Multiphase Flow, Volume 95, October 2017, Pages 71-83, doi: 10.1016/j.ijmultiphaseflow.2017.05.006.
17. E. Movahednejad, F. Ommi, K. Nekofar, Tarbiat Modares. Experimental Study of Injection Characteristics of a Multi-hole port injector on various Fuel Injection pressures and Temperatures. EPJ Web of Conferences 45, 01116 (2013). DOI: 10.1051/epjconf/20134501116.
18. S. Falfari, G. M. Bianchi, L. Pulga, C. Forte, " PWI and DWI Systems in Modern GDI Engine: Optimization and Comparison - Part II: Reacting Flow Analysis", SAE Technical paper 21PFL-0136*, SAE WCX 2021 Congress, Detroit: Michigan, USA*.
19. Matteo Ricci, PhD Thesis, University of Bologna, 2020, “Numerical Assessment of the Water Injection Application to GDI Engines”.
20. Han, R. and Reitz, R.: “A temperature wall function formulation for variable-density turbulent flows with application to engine convective heat transfer modeling”, *Int. J. Heat Mass Transfer* Vol. 40, No 3, pp. 613-625, 1997, doi: http://dx.doi.org/10.1016/0017-9310(96)00117-2.
21. Brusiani, F., Bianchi, G., and Tiberi, A., “Primary Breakup Model for Turbulent Liquid Jet Based on Ligament Evolution,” SAE Technical Paper 2012-01-0460, 2012, https://doi.org/10.4271/2012-01-0460
22. Pulga, L., Falfari, S., Bianchi, G.M., Ricci, M. et al., “Advanced Combustion Modelling of High BMEP Engines under Water Injection Conditions with Chemical Correlations Generated with Detailed Kinetics and Machine Learning Algorithms,” SAE Technical Paper 2020-01-2008, 2020, doi:10.4271/2020-01-2008 – Selected to appear in *SAE International Journal of Advances and Current Practices in Mobility*.

Contact Information

For further information/details please contact:

Dr. Stefania Falfari: stefania.falfari@unibo.it

Prof. Gian Marco Bianchi: gianmarco.bianchi@unibo.it